Journal of Alloys and Compounds 509 (2011) 57–60

Contents lists available at ScienceDirect

Journal of Alloys and Compounds

journal homepage: www.elsevier.com/locate/jallcom

On the mechanism of grain refinement in Al–Zr–Ti alloys

T.V. Atamanenko[a,*,1], D.G. Eskin[b], M. Sluiter[a], L. Katgerman[a]

[a] Delft University of Technology, Dept. Materials Science and Engineering, Mekelweg 2, Delft 2628CD, The Netherlands
[b] Materials Innovation Institute, Mekelweg 2, Delft 2628CD, The Netherlands

ARTICLE INFO

Article history:
Received 3 June 2010
Received in revised form 5 September 2010
Accepted 8 September 2010
Available online 17 September 2010

Keywords:
Aluminum alloys
Intermetallics
Nucleation
Grain refinement
Cavitation
Ultrasound

ABSTRACT

In high-strength aluminum alloys Ti and Zr are commonly present as alloying elements, mostly as anti-recrystallization agents. Grain refinement during solidification is also achieved using Ti but in the form of titanium borides. Our previous investigations showed that a combined addition of Zr and Ti enables considerable grain refinement in aluminum alloys upon cavitation treatment, much stronger than that of Zr alone. The role of titanium and ultrasonic processing remained unclear. In this paper we propose a mechanism of the grain refinement that includes structural changes in solidification sites, their refinement and initiation of heterogeneous nucleation at lower undercooling.

1. Introduction

There are many techniques of grain refinement available in casting practice of aluminum alloys. Currently it is commonly achieved through the addition of small amounts of Al–Ti–B master alloys [1]. This technique is easy to apply; however, it is not always suitable for all alloys due to agglomeration of borides. Besides, the grain refiners are expensive and their efficiency under typical casting conditions is very low—only some percents of titanium borides are acting as solidification sites [2]. Direct alloying with the elements that are known as efficient grain refiners, e.g. Ti and Sc, requires fairly large level of alloying, 0.15–0.35 wt%. That is why physical methods of grain refinement [3–6] are potentially attractive for the industry. Cavitation-aided grain refinement induced by ultrasonic melt treatment (UST) is one of them.

Previous investigations have clearly demonstrated that UST promotes grain refinement in different Al-based alloying systems [4–7]. Our investigations show that when applied in the solidification range of primary (Al), it results in fine grain structure in all systems studied [8]. However, it is more difficult to achieve the same result while treating in the liquid state. With the attempt to combine the efficient ultrasonic processing with the fluid state of the processed alloy, we studied the effect of UST on grain refinement of aluminum alloys containing additions of transition metals in concentrations above the peritectic point. It has been shown that additions of Zr (≥0.18 wt%) and Ti (≥0.015 wt%) enable considerable grain refinement under the influence of cavitation induced above the temperature of primary aluminum formation (Fig. 1), i.e. the grain refinement occurs when the processing is performed in the temperature range of primary solidification of Al_3Zr [9]. It was shown that the achieved grain refinement was due to the increased nucleating potency of solidification sites [9]. What makes this process commercially attractive is that the grain refinement can be achieved without additional alloying of some commercial aluminum alloys that already contain Zr and Ti in their standard composition, application of Al–Ti–B being not necessary.

It was suggested that nucleation potential of $Al_3(Zr,Ti)$ particles is increased due to ultrasonic-assisted fragmentation of Al_3Zr particles and their saturation with Ti [9]. Current paper is aimed to clarify the mechanism of cavitation-assisted grain refinement of aluminum alloys with Zr and Ti additions.

2. Experimental

To study the influence of Ti additions on the structure formation of primary intermetallics in Al–Zr–Ti alloys both in the presence and absence of ultrasonic field, X-ray measurements had to be performed, which required high concentration of intermetallics in the sample. Thus, the amount of transition metals was increased by five times as compared to the alloys investigated before [9], keeping Zr:Ti ratio the same. Two model aluminum alloys were studied: Al–1 wt% Zr and Al–1 wt% Zr–0.25 wt% Ti. The alloys were prepared using 99.95 wt% pure aluminum, Al–5 wt% Ti, and Al–6 wt% Zr master alloys. The chemical composition was verified by X-ray fluorescent analysis in a Philips X-ray spectrometer PW 2510 on the middle transversal cross section of all the samples.

The experimental setup for ultrasonic processing is described in detail in Ref. [10]. A 17.5 kHz magnetorestrictive transducer was used. The input power at the

* Corresponding author. Tel.: +31 0 15 278 2201; fax: +31 0 15 278 6730.
E-mail address: T.Atamanenko@tudelft.nl (T.V. Atamanenko).
[1] www.tudelft.nl.

0925-8388/$ – see front matter © 2010 Elsevier B.V. All rights reserved.
doi:10.1016/j.jallcom.2010.09.046

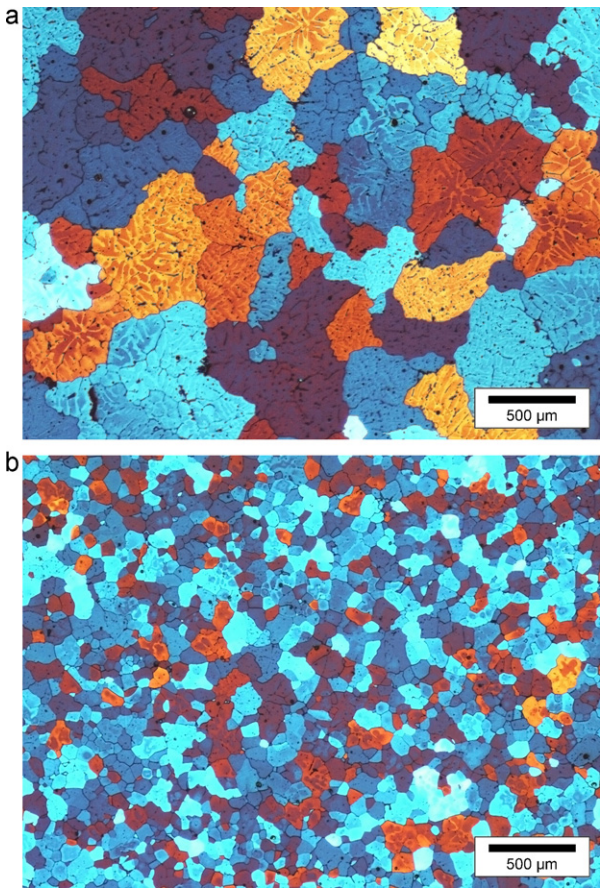

Fig. 1. Grain structures observed in ingot samples of an Al–0.18 Zr–0.06 mass% Ti alloy, (a) without and (b) with ultrasonic melt treatment.

generator was 4 kW. The amplitude of vibrations was measured in air on an ultrasonic horn with the help of a non-contact vibrometer. The amplitude of vibrations was 40 μm. The horn was made of niobium.

In each experiment, 350 g/180 cm^3 charge was melted in a stationary electric furnace at 930 °C and then poured into smaller pre-heated graphite cup-shaped crucibles (180 g/90 cm^3) where they were either treated with ultrasound or cooled in the presence of the idle ultrasonic horn down to 853 °C. The liquidus of an Al–1 wt% Zr alloy is 894 °C. The ultrasonic system was switched on before the horn was dipped into the liquid metal. The insertion depth of the ultrasonic horn was 3 mm below the surface of the liquid metal. Treatment time was about 10 s. After the treatment samples solidified in the graphite crucible. The cooling rate during solidification was 0.9 K/s.

All samples were sectioned transversally 10 mm above the bottom of the sample. The observations of the as-cast grain structures were made by conventional metallography (cutting, polishing down to 1 μm diamond paste, and electrolytic oxidation at 20 VDC in a 3% HBF_4 water solution) using a Neophot-31 optical microscope. The particle size was measured in the center of cast samples on photographs using random linear intercept technique. Statistical analysis of the results was performed.

Morphology and composition of primary intermetallic particles were examined in a scanning electron microscope JSM 6500F using back-scattered electron images and energy dispersive X-ray spectrum analysis (EDS). The Bruker-AXS (Siemens) D5005 wide-angle diffractometer was used to study the lattice parameters of structure constituents.

3. Results and discussion

There are several parameters that make the solidification site for heterogeneous nucleation efficient: low interfacial energy (realized through crystallographic match with the nucleating phase and good wetting) and the size matching the thermal undercooling. Let us look at our results with keeping in mind these parameters.

In this study we confirmed that cavitation facilitates dissolution and homogeneous distribution of Ti along the Al_3Zr particle length, as it has been reported earlier for smaller concentrations of Zr and Ti [9]. After solidification without cavitation the concentration of Ti in smaller particles (50–70 μm in size) changes along their length. In the center of the particle the concentration of Ti was about 5–6 at.%, while at the periphery it ranges from 8 to 11 at.%. The central part of larger particles (100–300 μm) does not contain any Ti, while at the periphery titanium concentration is about 4 to 10 at.%. When cavitation treatment is applied, the particles are refined to 30–50 μm and Ti is homogeneously distributed along the particles length. The concentration of Ti in the particles ranges from 5 to 12 at.%. Homogeneous distribution of Ti may be a result of smaller particle size and/or ultrasonic enhanced diffusion.

It is known that there is a good matching between the lattice parameters of aluminum and Al_3Zr particles, the overall mismatch is about 2.9% [11]. Obviously, our first hypothesis was that Ti being dissolved in Al_3Zr decreased the mismatch and improved the nucleation potential of $Al_3(Zr_{1-x}Ti_x)$ particles. However, according to the results of XRD investigations, the additions of Ti decrease the lattice parameters of DO_{23} structure in good agreement with reported data [12]. Fig. 2 represents the XRD scans of two discs made of Al–1 wt% Zr and Al–1 wt% Zr–0.25 wt% Ti alloys. The grey pattern (Al–1 wt% Zr alloy) matches well with the reflections of Al_3Zr standard data file, indicating that the sample contains DO_{23} structure (Al_3Zr). The reflections of Al–1 wt% Zr–0.25 wt% Ti alloy sample solidified both in the presence and in the absence of cavitation (black pattern) are identical and show somewhat larger diffraction angles. Its is known that the tetragonal equilibrium DO_{23} type structure ($Al_3(Zr_{1-x}Ti_x)$) exists in a wide range of compositions from pure Al_3Zr to x = 0.4 [13]. Ti substitutes Zr in the DO_{23} phase [13]. That is why the lattice parameters of the DO_{23} phase continuously vary along the Al_3Zr–Al_3Ti section of the phase diagram almost over the whole concentration range [12]. To match the reflections of the standard Al_3Zr data and the sample made of an Al–1 wt% Zr–0.25 wt% Ti alloy, the lattice parameters had to be adjusted. As a result, it was found that the lattice parameter a decreased from 0.4009 [14] to 0.3993 nm, while the c parameter is reduced from 1.728 nm [14] to 1.713 nm.

The lattice mismatch between two phases is defined as

$$\delta = \frac{2(a - a_0)}{a + a_0}. \quad (1)$$

If one compares a and $c/4$ interplanar distances of tetragonal $Al_3(Zr_{1-x}Ti_x)$ structure (DO_{23}) with the lattice parameter of FCC aluminum at room temperature, which is equal to 0.40496 nm [12], it is clear that Ti additions only increase the mismatch between a parameter of $Al_3(Zr_{1-x}Ti_x)$ structure and aluminum from 1 to 1.4%. The mismatch between $c/4$ and aluminum is decreased from 6.5 to 5.6%, however it is still too high to promote nucleation along this plane. Taking into the account that aluminum expands at higher temperatures ($\alpha = 34.3 \times 10^{-6}\ K^{-1}$, a = 0.4124 nm at 660 °C [15]) to

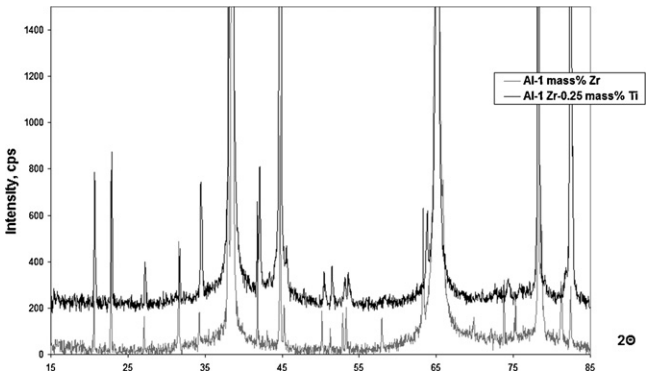

Fig. 2. XRD scans of Al–1 mass% Zr and Al–1 Zr–0.25 mass% Ti discs solidified without cavitation treatment.

a larger extent than the DO_{23} phase ($\alpha = 15–16 \times 10^{-6}\ K^{-1}$ [16]), the mismatch between a parameter of $Al_3(Zr_{1-x}Ti_x)$ structure and FCC aluminum increases to 2.4%, while the mismatch between $c/4$ of Al_3Zr and a of aluminum is decreased to 4.5%. We can conclude that our hypothesis was wrong as the increase of the lattice mismatch between aluminum and the DO_{23} structure is supposed to decrease the nucleation potential of the $Al_3(Zr_{1-x}Ti_x)$ particles.

On the other hand, when the lattice mismatch increases it results in higher interfacial energy between $Al_3(Zr_{1-x}Ti_x)$ particles and aluminum. The solid/liquid interfacial energy σ is in direct proportion to the nucleation undercooling ΔT:

$$\Delta T = \frac{4\sigma}{\Delta S_v d}, \quad (2)$$

where ΔS_v is the entropy of fusion per unit volume and d is the particle diameter [17]. It means that higher interfacial energies promote a higher energy barrier for nucleation and thus, a higher undercooling is required. It has been shown experimentally, that nucleation occurs on the largest particles first [18]. At lower undercooling, smaller particles become active [17]. The mechanism of enhanced nucleation by $Al_3(Zr_{1-x}Ti_x)$ particles may be by delayed nucleation when less potent but smaller $Al_3(Zr_{1-x}Ti_x)$ particles are activated.

As it has been already mentioned, cavitation melt treatment facilitates refinement of primary intermetallics, which is in agreement with previous observations [5,9]. Fig. 3a represents the microstructure of a model Al–1 wt% Zr alloy without UST. The size of Al_3Zr particles varies between 100 and 300 μm. After adding 0.25 wt% Ti two types of particles were found, with size ranging: (1) 50–70 μm and (2) 100–300 μm. When UST is applied, the particles become considerably smaller in size, in the range of 30–50 μm (Fig. 3c). According to the nucleation theory, refinement of primary intermetallics increases the amount of potential solidification sites that still have to be activated by undercooling [17,19]. Particles of about 100–300 μm require an undercooling of 0.002–0.006 K to be active as nucleation sites according to Eq. (2). When particles size is decreased to 30–50 μm, the required undercooling is larger, about 0.011–0.019 K. The experiments on Al–1 wt% Zr–0.25 wt% Ti alloy have shown that cavitation melt treatment does not lead to considerable grain refinement. The grain size was only reduced from 130 to 110 μm due to the fact that solidification sites (intermetallics fragmented by cavitation) were still very large. When the size of intermetallics was less than 3–5 μm (in an Al–0.2% Zr–0.06% Ti alloy), which corresponds to the undercooling of 0.11–0.19 K, the grain size was reduced from 140 to 40 μm (Fig. 1) [9]. These values of undercooling are significantly larger, but still within the range observed in casting practice, usually about 0.2 K [20]. The growth restriction caused by titanium dissolved in liquid aluminum can further enhance the grain refining effect in Al–Zr–Ti alloys, but this effect seems to be secondary to the refinement of $Al_3(Zr, Ti)$ particles, modification of their structure, and the delay in the nucleation to larger undercooling. In our previous paper [9] we have demonstrated that the addition to Al–Zr alloys of V, which is also strong growth restricting element, does not produced any grain refinement upon ultrasonic melt treatment despite the refinement of Al_3Zr particles.

Structure observations apparently demonstrate that Ti additions promote cracking of $Al_3(Zr_{1-x}Ti_x)$ particles, facilitating their fragmentation by cavitation treatment. Fig. 3b shows $Al_3(Zr_{1-x}Ti_x)$ particles with multiple cracks. XRD measurements have demonstrated that the reflections of the samples with Ti additions, with and without cavitation treatment, exhibit appreciable line broadening (Fig. 2), which might be an evidence of an increased internal stress due to dissolved Ti that promotes fragmentation of particles.

We have mentioned in the beginning of the paper that wetting could be one of the mechanisms to enhance the nucleating potency

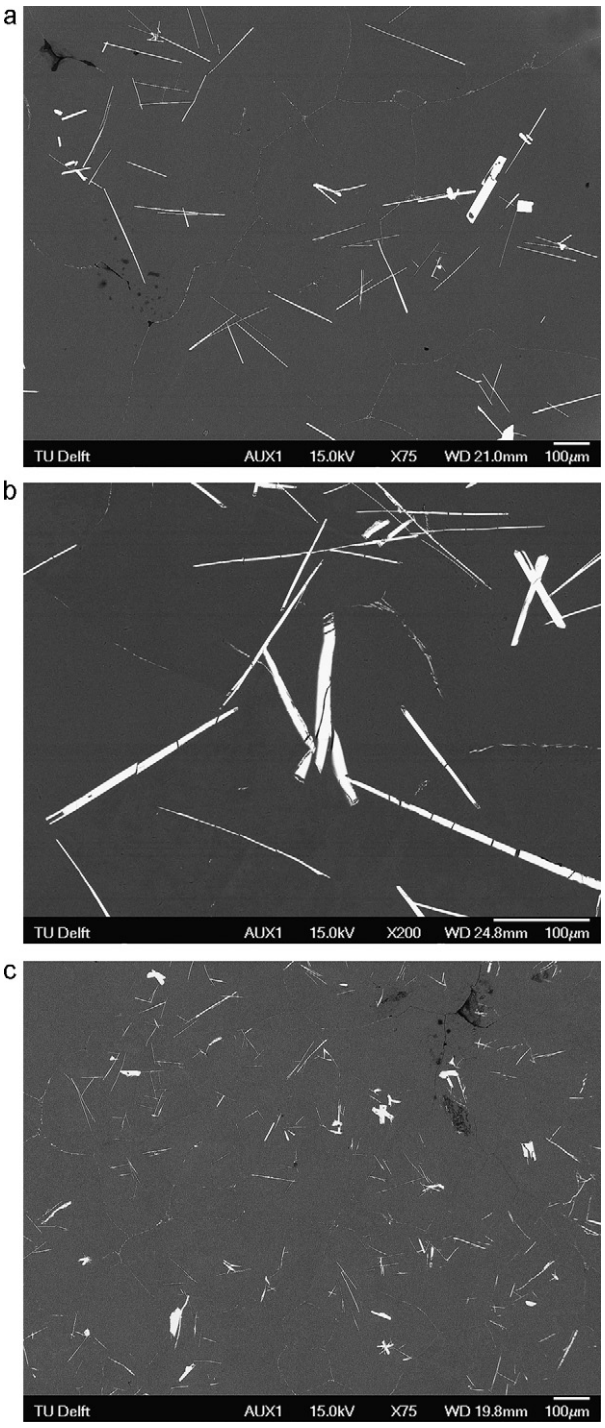

Fig. 3. Morphology of primary intermetallics in: (a) an Al–1 mass% Zr alloy without UST; (b) in an Al–1 mass% Zr–0.25 mass% Ti alloy without cavitation treatment, note higher magnification; and (c) an Al–1 mass% Zr–0.25 mass% Ti alloy with UST.

of a substrate. Cavitation treatment indeed is known to facilitate the wetting, e.g. of oxide particles in liquid aluminum [5]. In our particular case of Al–Zr system, wetting should not be an issue as the Al_3Zr phase (with or without dissolved Ti) is naturally formed in the system, being perfectly indigenous. Another phenomenon that is known to accompany cavitation is the local undercooling in the vicinity of a collapsing cavitation bubble [5,6]. This should result in activation of yet smaller particles, facilitating further grain refinement. On top of this, acoustic streaming produced by UST enables even distribution of refined primary intermetallics in the whole melt volume [5,6].

Thus, based on the experimental findings and general consideration of the nucleation theory [17], the following mechanism for the grain refinement effect in Al–Zr–Ti alloys produced with cavitation treatment in the temperature range of solidification of primary intermetallics can be suggested. Cavitation melt treatment applied above the temperature of primary aluminum formation promotes fragmentation of Al_3Zr particles (stable DO_{23} structure, with high melting point [12]), decreases the size of potential solidification sites, and increases their number. At the same time, Ti substitutes Zr in $Al_3(Zr_{1-x}Ti_x)$ particles, increasing the interfacial energy between aluminum and $Al_3(Zr_{1-x}Ti_x)$ particles, which leads to the delay of nucleation to larger undercooling. If the undercooling is increased, the critical radius decreases. In this way Ti delays the nucleation to the temperature when smaller $Al_3(Zr_{1-x}Ti_x)$ particles, previously refined by cavitation, can be activated. Collapse of cavitation bubbles may further contribute to the undercooling and, therefore to activation of even smaller particles.

It is supposed that the tendencies, which were observed on aluminum alloys with high concentration of Zr and Ti and reported in this paper, are also correct for smaller amounts of additions with the same Zr:Ti ratio, resulting in the observed grain refinement [9].

Acknowledgements

The authors wish to thank Dr. A.J. Böttger, Dr. R. Delhez and N.M. van der Pers for the help with XRD investigations. This work is performed within the framework of Research Program of the Materials Innovation Institute (www.m2i.nl), project MC4.05215.

References

[1] B.S. Murty, S.A. Kori, M. Chakraborty, Int. Mater. Rev. 47 (2002) 3.
[2] I. Maxwell, A. Hellawell, Acta Metall. 23 (1975) 229.
[3] D.K. Chernov, Proceedings of the Imperial Russian-Technical Society, St. Petersburg, 1, 1879, p. 1.
[4] C. Vives, J. Cryst. Growth 158 (1998) 118.
[5] G.I. Eskin, Ultrasonic Treatment of Light Alloy Melts, Gordon and Breach Science Publishers, Amsterdam, The Netherlands, 1998.
[6] O.V. Abramov, Ultrasound in Liquid and Solid Metals, CRC Press, Boca Raton, FL, 1994.
[7] H.J. von Seemann, H. Staats, K.G. Pretor, Arch. Eisenhutt. 38 (1967) 257.
[8] T.V. Atamanenko, D.G. Eskin, L. Katgerman, Int. J. Cast Met. Res. 22 (2009) 26.
[9] T.V. Atamanenko, D.G. Eskin, L. Zhang, L. Katgerman, Metall. Mater. Trans. A 41A (2010) 2056.
[10] T.V. Atamanenko, D.G. Eskin, L. Katgerman, in: J. Hirsch, B. Skrotzki, G. Gottstein (Eds.), Aluminum Alloys: Their Physical and Mechanical Properties, vol. 1, Wiley-VCH, Weinheim, Germany, 2008, pp. 315–320.
[11] M. Zedalis, M.E. Fine, Scripta Metall. 17 (1983) 1247.
[12] L. Tretyachenko, Al–Ti–Zr, in: G. Eftenberg, S. Ilyenko (Eds.), Ternary Alloy Systems: Phase Diagrams, Crystallographic and Thermodynamic Data, subvolume A, part 4, Springer, Berlin, 2006, pp. 54–67.
[13] M.V Karpets, Yu.V. Milman, O.M. Barabash, N.P. Korzhova, O.N. Senkov, D.B. Miracle, T.N. Legkaya, I.V. Voskoboynik, Intermetallics 11 (2003) 241.
[14] S. Srinivasan, P.B. Desch, R.B. Schwarz, Scripta Metall. 20 (1991) 2513.
[15] K. Wang, R.R. Reeber, Philos. Mag. A 80 (2000) 1629.
[16] R.A. Varin, Metall. Mater. Trans. A 33A (2002) 193.
[17] A.L. Greer, A.M. Bunn, A. Tronche, P.V. Evans, D.J. Bristow, Acta Mater. 48 (2000) 2823.
[18] A. Tronche, A.L. Greer, Philos. Mag. Lett. 81 (2001) 321.
[19] M.C. Flemings, Solidification Processing, McGraw-Hill, New York, 1974.
[20] T.E. Quested, A.L. Greer, Acta Mater. 52 (2004) 3859.